CROATICA CHEMICA ACTA
CCACAA **79** (1) 15–25 (2006)

ISSN-0011-1643
CCA-3060
Original Scientific Paper

Comparative Evaluation of Scanned Stripping Techniques: SSCP *vs.* SSV*

Raewyn M. Town[a,] and Herman P. van Leeuwen[b]**

[a]*Department of Chemistry, University of Southern Denmark, Campusvej 55, DK-5230 Odense, Denmark*

[b]*Laboratory of Physical Chemistry and Colloid Science, Wageningen University, Postbus 8038, Dreijenplein 6, 6703 HB Wageningen, The Netherlands*

RECEIVED MAY 30, 2005; REVISED JUNE 24, 2005; ACCEPTED JUNE 28, 2005

The characteristic features of scanned deposition potential curves constructed from stripping chronopotentiometry (SSCP) and various modes of stripping voltammetry (SSV) are critically evaluated. The strengths and weaknesses of each method for identification of metal ion speciation features and susceptibility to typical interferences are described for conventional (HMDE) and microelectrodes, *i.e.* irreversibility in the electron transfer reaction, multi-metal resolution, intermetallic compound formation, homogeneous kinetics, induced metal adsorption, and requirement for excess ligand to avoid saturation at the electrode surface during reoxidation. The most advantageous stripping modes are those in which practically complete depletion of the accumulated metal is achieved during the reoxidation step, *i.e.* SCP with low stripping current and DC-SV with slow potential scan rate. Under these conditions there is a straightforward quantitative relationship between the amount of metal accumulated and the analytical signal. The slow rate of oxidation with these modes renders them practically immune to induced metal adsorption; they have a lower requirement for excess ligand in the sample solution and greater resistance to both irreversibility in the electrochemical oxidation and to interference from intermetallic compounds. Even in the case of nonreversible electrode processes, or for systems limited by complex formation/dissociation kinetics, depletive scanned deposition potential stripping curves allow complexation parameters to be determined from the shift in half-wave deposition potential, analogous to the DeFord-Hume approach for conventional voltammetry. SSCP has greater sensitivity, and provides greater resolution in multi-metal systems than does depletive DC-SSV, while SSV provides useful complementary information in some cases.

Keywords
stripping chronopotentiometry
stripping voltammetry
metal speciation
microelectrode
irreversibility
heterogeneity

INTRODUCTION

Electrochemical stripping techniques that employ a preconcentration step have found widespread application in analysis of trace metal speciation in environmental media.[1] Two-steps are comprised: a deposition step during which for a fixed period of time metal ions are reduced at a constant potential, followed by a quantification step involving reoxidation of the accumulated metal. In stripping voltammetry (SV) oxidation is effected by application of an anodically ramping potential and the analytical signal is the resulting current recorded as a function

* Dedicated to the memory of the late Professor Marko Branica.

** Author to whom correspondence should be addressed. (E-mail: rmt@chem.sdu.dk)

of applied potential. The maximum current (peak height) is taken as proportional to the amount of metal accumulated. Various potential waveforms are employed with square wave (SW) being favoured for its rapidity and sensitivity.[1] In stripping chronopotentiometry (SCP) the accumulated metal is quantified by application of a constant oxidising current, or flux of a chemical oxidant, and the analytical signal is the time taken for reoxidation, the transition time, τ. Reliable determination of τ is readily achieved by measuring the area under the peak in the dt/dE *vs. E* plot, where dt/dE denotes the inverse of the time derivative of the recorded potential.[2] For a sufficiently low oxidising current, essentially complete depletion of the accumulated metal from the electrode is achieved, and this depletive SCP regime has the greater sensitivity and resolution.[2]

In single deposition potential methods, complexation parameters are determined from the changes in stripping peak magnitude and potential under limiting current conditions, *i.e.* for deposition potentials well negative of the reduction potential of the target metal. However, such comparisons have limited utility: transient stripping peaks (SV or SCP) are subject to secondary effects, including disproportional enhancement due to induced metal ion adsorption,[3] and broadening/splitting with reduced potential shifts due to ligand saturation during stripping.[4–7] Depletive SCP is practically not affected by induced metal adsorption[8,9] and has a significantly lower requirement for excess ligand at the electrode surface during reoxidation (which, in contrast to SV, is independent of t_d).[6,8] The stripping peak half-width of *ca.* 20 mV[10] is much narrower than that for the various SV modes (range 45–65 mV) thus providing better resolution[11] in multimetal solutions. Yet, whilst the surface area of the depletive SCP peak, usually in dt/dE *vs. E* format, provides a straightforward quantitation of the accumulated metal, interpretation of speciation parameters from individual peaks is involved.[10] Also, the position of the peak is dependent on the concentration of metal accumulated during the deposition step due to the influence of the concentration of reduced metal in the electrode volume on the equilibrium potential at the end of the deposition time.[10]

Complete voltammetric potential-current curves are inherently richer in information content than the individual stripping peaks resulting from accumulation at limiting deposition current conditions. As the measurements are made from the foot of the wave to the limiting deposition current region the relevant part of the stability distribution and corresponding parts of the rate constant distributions are scanned.[12] Conventional DC steady-state voltammetry lacks the necessary sensitivity for measurements at environmentally relevant concentrations, however, analogous curves can be constructed by plotting the magnitude of the electrochemical stripping peak as a function of deposition potential, E_d. Bubić and Branica first proposed this approach for DC-SV which they termed 'pseudopolarography'.[13] We have coined the more representative terminology scanned (deposition potential) stripping voltammetry (SSV), and similar curves using chronopotentiometric oxidation, we denote as SSCP. Although SSCP and SSV waves are basically different from conventional steady-state voltamograms, speciation parameters derive from the change in the half wave deposition potential, $E_{d,1/2}$, that occurs on complexation, and the magnitude of the limiting plateau, analogous to the DeFord-Hume expression for voltammetric waves,[14] so long as no secondary effects are operative. Recording of SSV and SSCP waves is evidently more time consuming than conventional voltammetric measurements, but the process is easily automated.[15,16] SSV, most often in DP- or SW-mode, has been successfully used for determination of metal ion complexation parameters for simple ligands,[17–21] whilst its application to natural waters typically results in poorly defined waves,[22–26] and data interpretation has been rather empirical.

Any deposition-related complications that may occur in SV will also be problematic for SCP. These include (i) formation of intermetallic compounds such as Zn/Cu,[11,27] (ii) insufficient ligand excess during the accumulation step resulting in variation of the mean diffusion coefficient over the diffusion layer,[28,29] and (iii) the need to buffer solutions in certain cases to avoid pH changes at the electrode surface.[30]

Here we discuss the characteristic features of SSCP *vs.* SSV waves and their utility for trace metal speciation analysis. The influence of various effects on the wave shape, such as induced metal adsorption, heterogeneity in the chemical speciation, and irreversibility in the electron transfer step are characterised. We highlight the different features for nondepletive *vs*. depletive stripping conditions. This distinction is analytically important: under depletive conditions there is a direct quantitative relationship between the total amount of metal accumulated and the analytical signal. This feature is lacking for nondepletive modes which are accordingly of limited utility for determination of metal speciation parameters, restricted to a certain set of metal-ligand systems and experimental conditions. For SV, complete depletion can be attained by use of a very slow DC scan rate,[11,31,32] with the integrated current (peak area) being taken as the analytical signal. However, this mode has relatively low sensitivity, and practical SV measurements are typically of a nondepletive nature, relying on the peak height for quantitation. For SSCP complete depletion is easily attained by use of a sufficiently low stripping current, and offers sensitivity comparable to that for DP-SV.[2]

EXPERIMENTAL

Reagents

All solutions were prepared in distilled, deionised water (resistivity > 18 MΩ cm). Cu^{II}, Pb^{II}, Cd^{II}, and Zn^{II} solu-

tions were prepared by dilution of commercial certified standards. KNO_3 solutions were prepared from solid KNO_3 (BDH, AnalaR). Acetate buffer, pH = 4.8, was prepared by combining acetic acid (Prolabo, Rectapur) and sodium acetate (Janssen Chimica, pure). Pyridine-2,6-dicarboxylic acid (PDCA) was from Fluka (purum). Fulvic acid was the standard peat fulvic acid from the International Humic Substances Society (1S103F).

Solutions were initially purged with oxygen-free nitrogen, then a nitrogen blanket was maintained during measurements. Measurements were performed at 20 °C.

Apparatus

An Ecochemie μ-Autolab or PGSTAT10 potentiostat was used in conjunction with a Metrohm 663 VA stand. The electrometer input impedance of these instruments is $>10^{11}$ Ω. The working electrode was a Metrohm multimode mercury drop electrode (surface area, $A = 5.2 \times 10^{-7}$ m^2; Aldrich, ACS reagent mercury, 99.9995 %), the auxiliary electrode was glassy carbon, and the reference electrode was Ag|AgCl|KCl (sat) encased in a 0.1 mol dm^{-3} KNO_3 jacket. All data presented are raw data, *i.e.* no smoothing procedures were applied.

RESULTS AND DISCUSSION

General Theory

The theory for SSCP has been detailed previously.[33–35] The main principles, which are equally applicable to SSV under depletive stripping conditions, are recalled briefly herein. Except in the limiting case of a completely irreversible system,[34] at a given deposition potential, E_d, the deposition current, I_d, is a function of time, and its relationship with the concentration of reduced M in the electrode, $c^*_{M^0}$, must take the form of an integral.[33] The evolution of I_d with deposition time is shown in Figure 1 for several degrees of reversibility. As the accumulation step proceeds, $c^*_{M^0}$ increases from 0 at $t = 0$ to values much greater than the bulk solution metal ion concentration, c^*_M, at $t = t_d$.

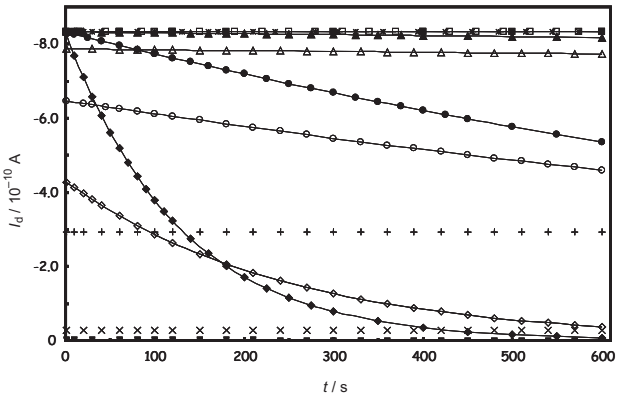

Figure 1. The deposition current, I_d, calculated as a function of time, t, at various deposition potentials, E_d, for reversible, quasi-reversible, and irreversible systems. Values are calculated for an electrochemical reaction which is (i) reversible ($k^o = \infty$): E_d / V = –0.80 (■); –0.53 (▲); –0.49 (●); –0.46 (◆), (ii) quasi-reversible ($k^o = 5 \times 10^{-6}$ m s^{-1}): E_d / V = –0.80 (□); –0.53 (△); –0.49 (○); –0.46 (◇), and (iii) irreversible ($k^o = 1 \times 10^{-8}$ m s^{-1}): E_d / V = –0.80 (∗); –0.60 (+); –0.53 (×); –0.49 (- -). In each case values were calculated for a HMDE ($A = 5.2 \times 10^{-7}$ m^2, $V = 3.5 \times 10^{-11}$ m^3, $\delta = 2 \times 10^{-5}$ m) at $T = 293$ K, for a metal with $D = 8.3 \times 10^{-10}$ m^2 s^{-1}, $E^o = -0.405$ V, and $c^*_M = 2 \times 10^{-7}$ mol dm^{-3}.

Under depletive stripping conditions the concentration of reduced M at the surface of the electrode, $c^0_{M^0}$, is practically equal to $c^*_{M^0}$ and this allows us to ignore consideration of the flux and concentration gradient of M^0 inside the small spherical electrode volume. Furthermore, in depletive SCP, c^0_M remains approximately constant with time because the applied current generates a constant gradient of M and the volume of the medium is usually large enough to warrant an essentially invariant c^*_M.

Previous analysis of SSV waves has been incorrectly formulated. Shuman and Cromer[36] expressed the deposition flux into the electrode in terms of semi-infinite planar diffusion, confusing the mean concentration of M^0 with a virtual bulk concentration outside the diffusion layer. Others have derived expressions on the basis of a linear proportionality between $c^*_{M^0}$ and some steady-state deposition current;[37,38] the ensuing equations for the SSV waveform are thus essentially meaningless. Our integral treatment results in a rigorous equation that fully describes the relationship between the stripping time, τ, and the deposition potential E_d, at both a conventional HMDE and a microelectrode in the complete depletion regime:[33]

$$\tau = \frac{I^*_d \tau_d}{I_s} [1 - \exp(-t_d / \tau_d)] \qquad (1)$$

where τ_d is the characteristic time constant for the deposition process. The time constant for attainment of steady-state, in both the deposition and stripping steps, is typically negligible relative to the measurement timescale. Thus transient effects related to establishment of a constant diffusion layer thickness[39] can be ignored. Eq. (1) is fully applicable to the quasireversible and irreversible cases, with more involved expressions for τ_d and I^*_d (see below).[34] An important feature of Eq. (1) is that it is explicit in the analytical signal, τ: this straightforward relationship holds only for depletive stripping techniques, and would be applicable only in exceptionally ideal cases to transient modes.

Eq. (1) shows that for a reversible system the depletive stripping waves have a form basically different from conventional voltamograms. They do not conform to a linear log-plot and are distinctly steeper. Furthermore, they lie to more negative potentials, even more so at a microelectrode, due to the influence of $c^*_{M^0}$ on the equilibrium potential, E_{eq}, at $t = 0$.[10] Figure 2 compares the scanned deposition potential stripping waves for depletive conditions and conventional voltamograms for reversible, quasi-reversible and irreversible systems at a HMDE and a microelectrode. The shapes are a direct consequence of the

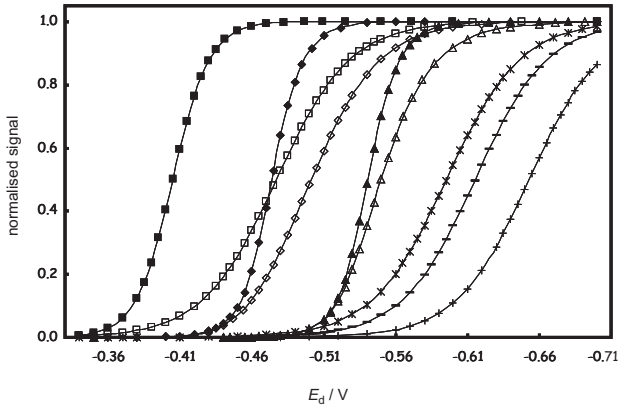

Figure 2. Scanned deposition potential deposition stripping curves calculated for depletive conditions at a HMDE and a microelectrode, in comparison with a conventional voltamograms. Curves are shown for a system which is (i) reversible ($k^\circ = \infty$) for a conventional voltamogram (■), HMDE (◆), microelectrode (▲), (ii) quasireversible ($k^\circ = 1 \times 10^{-6}$ m s^{-1}) for a conventional voltamogram (□), HMDE (◇), microelectrode (△), and (iii) irreversible ($k^\circ = 1 \times 10^{-8}$ m s^{-1}) for a conventional voltamogram (∗), HMDE (–), microelectrode (+). The voltamogram was calculated for $t = 1$ s, conditions for the HMDE were $A = 5.2 \times 10^{-7}$ m^2, $V = 3.5 \times 10^{-11}$ m^3, $\delta = 2 \times 10^{-5}$ m, and for the microelectrode $r_0 = 4.5 \times 10^{-6}$ m, $A = 1.3 \times 10^{-10}$ m^2, $V = 1.9 \times 10^{-16}$ m^3. Other parameters in each case: $D = 8.3 \times 10^{-10}$ m^2 s^{-1}, $E^\circ = -0.405$ V, $\alpha = 0.5$, $T = 293$ K.

I_d *vs.* t dependencies (Figure 1). Quasireversible and irreversible systems are discussed below.

Practical measurement of each SV stripping peak for construction of an SSV wave requires use of a common initial potential, sufficiently negative of the reoxidation peak potential, that is applied immediately prior to the stripping step.[15] For SCP this step is not necessary and the oxidation current can be applied directly from each E_d. The ability to avoid use of an initial potential is a significant advantage of SSCP. Figure 3 shows the SSCP waves with and without application of a common initial potential prior to measurement of each SCP peak (applied for the duration of the equilibration time, 10 s). The relative contribution from deposition during the equilibration time is greatest for the lower t_d values. Furthermore, Figure 3 demonstrates that a simple correction, comprised of subtracting the baseline value at the more positive E_d from all data points, is not valid; the impact of this effect decreases from the foot to the plateau of the wave. This effect can be minimised for speciation measurements by SSV by use of long t_d, however in practice this is limited by the requirement for excess ligand during reoxidation.

Multi-metal Systems

In multi-metal systems we must consider potential interferences that could arise within the preconcentrated mixture in the electrode, *e.g.* intermetallic compound formation, and during the oxidation step, *e.g.* one metal affecting the mode of detection of another, and the ability to resolve the signals for each metal. For the latter aspect, the very narrow depletive SCP peaks provide resolution far superior to that of SV; Figure 4.

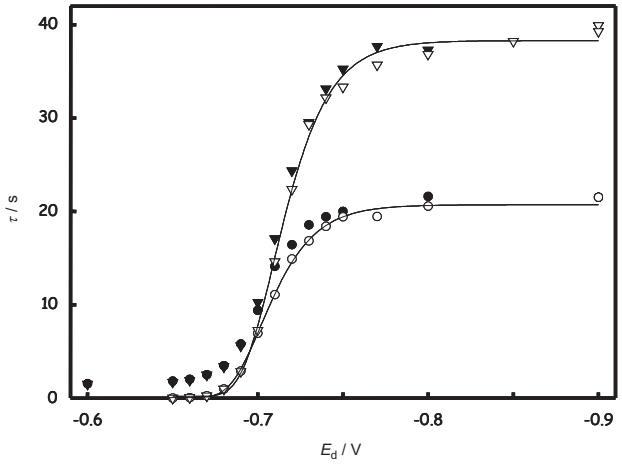

Figure 3. Experimental SSCP waves for Cd^{II} showing the effect of using a common initial potential to record each constituent stripping peak. Open symbols are for application of I_s directly from each E_d; closed symbols use a common initial potential of –0.90 V for the rest period duration. Data are shown for a deposition time, t_d, of 60 s (○,●) and 120 s (▽,▼). Conditions: HMDE ($A = 5.2 \times 10^{-7}$ m^2, $V = 3.5 \times 10^{-11}$ m^3), rest period = 10 s; $I_s = 2 \times 10^{-9}$ A; $c^*_{Cd^{II}} = 2 \times 10^{-7}$ mol dm^{-3} in 0.1 mol dm^{-3} KNO_3, pH = 4.8, $T = 293$ K.

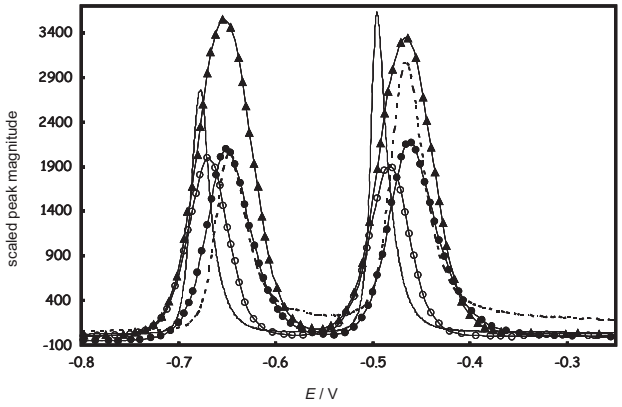

Figure 4. Stripping peaks measured in mixed Cd^{II} and Pb^{II} solution for various modes of SCP and SV. Data are shown for SCP in depletive ($I_s = 2 \times 10^{-9}$ A) (—), and nondepletive mode ($I_s = 1 \times 10^{-7}$ A) (- -), and for SV: DC (●); DP (○), and SW (▲). Conditions: HMDE, $t_d = 300$ s, $E_d = -0.90$ V, $c^*_{Cd^{II}} = c^*_{Pb^{II}} = 2 \times 10^{-7}$ mol dm^{-3} in 0.1 mol dm^{-3} KNO_3, pH = 4.8, $T = 293$ K. Other parameters: DC scan rate 10 mV s^{-1}; DP modulation amplitude 25 mV; SW frequency 50 Hz. Data are scaled on the *y*-axis to facilitate direct comparison.

SV and SCP have a common deposition step, and thus an equivalent susceptibility to interference from formation of intermetallic compounds. The presence of these compounds has a distinctive impact on the shape of the SSCP and SSV waves: the foot of the wave follows that for the intermetallic-free case, then once E_d is

sufficiently negative to generate the reduced metal concentrations in the electrode at which intermetallic compound formation occurs, the stripping signal decreases and a constant plateau is not attained.[11] The E_d at which the signal decrease is observed is more negative for depletive SSCP than for SSV. The resistance to interference from this phenomenon by depletive SSCP is ascribed to the slow oxidation rate: as the metal concentration in the electrode decreases during reoxidation, the intermetallic compound may have sufficient time to dissociate or redissolve, at least to some extent, within the mercury phase.[11] It is useful to note that dissociation of mercury soluble CuZn associates occurs with a half time of the order of 1 s,[40] which is relatively fast as compared to the timescale for depletive oxidation, but rather slow compared to transient SV modes.

At very high metal concentrations (far exceeding those usually encountered in environmental systems), electroless oxidation can interfere with SCP measurements.[11] That is, during the stripping step, whilst the potential is at a value corresponding to oxidation of a given metal, the ongoing incoming flux of less electropositive metal ions will contribute to the oxidation flux. This phenomenon leads to reduced SCP signals: the larger is the incoming metal ion flux, the greater must be the oxidation flux in order to be consistent with the constant applied I_s. The impact of this effect depends on the relative magnitudes of the metal fluxes and thus on the electrode size (see below); the shape of the SSCP wave is not affected. SV signals are not perturbed by this phenomenon because there is no prescribed net oxidation flux, and thus the constant current for ongoing reduction processes is contained within the SV baseline. As a corollary to these phenomena, both of which reduce the SCP signal, a high concentration of a more electropositive metal can result in a greater time available for ongoing deposition of less electropositive ones, and thus in enhanced signals. Again, the constant potential scan rate of SV renders it immune to this interference (which in any case can be avoided in SCP by selection of a less negative E_d to study the less electropositive metal).

The distinct features of SSCP and SSV in multi-metal systems renders their application complementary: the presence of electroless oxidation (a stripping step phenomenon) can be distinguished from intermetallic compound formation (arising during the deposition step). In any case, effects are only observed at relatively high metal concentrations.

Features in Labile Complex Systems

In Eq. (1), I_d^* plays the role of a form factor and an explicit expression for the shift in $E_{d,1/2}$ upon complexation can be derived from the exponential term only,[33] consistent with the DeFord-Hume approach for conventional voltammetry.[14] In the presence of a ligand forming labile complexes, ML, the terms in Eq. (1) are modified to include the complexation constant K' (= Kc_L), the diffusion coefficient of ML, and the corresponding diffusion layer thickness.[33,41] The shift in deposition potential, $\Delta E_{d,1/2}$, is given by:

$$\Delta E_{d,1/2} = -(RT / nF) [\ln(1+K') + \ln(\overline{D}/D_M)^p] \quad (2)$$

where $\overline{D}$ is the average diffusion coefficient for metal species (= $(D_M c_M^* + D_{ML} c_{ML}^*) / c_{M,t}^*$) and p is unity for a microelectrode and between 1/3 and 1/2 for a macroelectrode. At this point we note that such interpretation is possible because the shape of the SSCP wave is not altered in the presence of ligand.

For simple, well-characterised labile metal complex systems that are free from adsorption effects, *e.g.* Cd^{II}-pyridine-2,6-dicarboxylic acid, and under conditions of sufficient ligand excess, SSCP (depletive and nondepletive) and the various modes of SSV (DC, DP, and SW) all give comparable results.[42] That is, the shift in $E_{d,1/2}$ upon complexation is consistent with that predicted from the known stability constants, and there is no change in the slope of the wave. In case of insufficient ligand excess, the transition time for depletive SCP will still provide a correct measure of the amount metal accumulated. Thus SSCP waves recorded under conditions for which the reoxidation flux of M is greater than the maximum diffusive supply flux of L towards the surface will still be representative of the steady-state flux of M and the shift in $E_{d,1/2}$ has the value given by Eq. (2).[42] Under equivalent conditions, nondepletive SSV curves have no useful meaning since the peak height is no longer a reliable measure of the amount of metal accumulated.[6]

Features in Complex Systems with Limited Association/Dissociation Rates

In the case of kinetic currents, invoking the Koutecký-Koryta approximation[43–45] allows a rigorous expression to be obtained for the full SSCP wave.[35] This approach is based on the spatial division of concentration profiles for M and ML in the diffusion layer into a nonlabile and a labile region, separated by the boundary of the reaction layer with thickness, μ (=$(D_M / k_a c_L^*)^{1/2}$).[46] It amounts to including an operational lability criterion, $\mathscr{L}$, in the terms in Eq. (1), where $\mathscr{L}$ expresses the ratio between the kinetic and diffusive fluxes. For $\mu < x < \delta$, the system is considered as labile ($\mathscr{L} >> 1$), implying that there is equilibrium between M and ML, and ML contributes fully to the flux via coupled diffusion with M. For $0 < x < \mu$ the system is nonlabile ($\mathscr{L} << 1$) and the contribution from ML is purely kinetic. Systems with limited association/dissociation rates have an initially smaller I_d (Figure 5) and longer deposition time constant, τ_d. SSCP waves for the quasilabile CdNTA system, at conventional and microelectrodes, are well described by this approach.[35] The

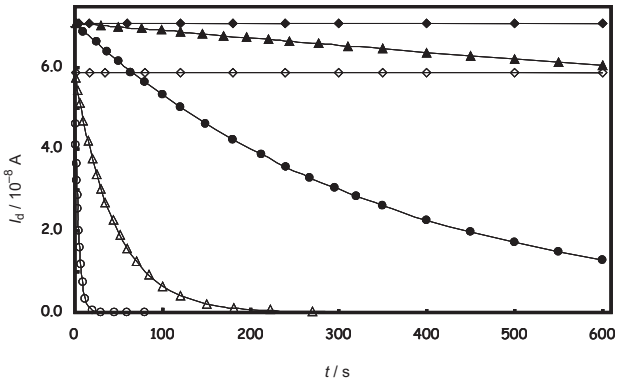

Figure 5. The deposition current, I_d, calculated as a function of time, t, at various deposition potentials, E_d, for systems which are labile (solid symbols) and quasi-labile (open symbols). Data are shown for E_d / V = –0.90 (◆,◇) –0.74 (▲,△) and –0.71 (●,○). Values were calculated for a HMDE ($A = 5.2 \times 10^{-7}$ m^2, $V = 3.5 \times 10^{-11}$ m^3), $E° = -0.586$ V, $D_M = D_{ML} = 7 \times 10^{-10}$ m^2 s^{-1}, T = 293 K, $c^*_M = 2 \times 10^{-7}$ mol dm^{-3}, $c^*_L = 10^{-4}$ mol dm^{-3}, $K_{ML} = 10^6$ dm^3 mol^{-1}, $k_a = 4.05 \times 10^9$ dm^3 mol^{-1} s^{-1}, $\mu = 4.16 \times 10^{-6}$ m, $\delta = 2 \times 10^{-5}$ m.

limiting τ is lower than that for the fully labile case, even more so at a microelectrode due to enhanced diffusion.[47] Yet the log slope is not modified,[35] and the stability constant can be obtained from the shift in $E_{d,1/2}$ by including a term ($\ln(\tau_{ML}/\tau_M)$) that accounts for the positive shift in the wave position due to the reduced lability.[48]

Effects of Induced Metal Adsorption

For not too high adsorption coefficients (Henry coefficient, K_H, less than *ca.* 10^{-4} m), the diffusive time constant for the adsorptive process, τ_{ad} (= $K_H \delta / D$ for convective diffusion during deposition), is short compared to practical t_d values. This implies that adsorbed metal species generally have no significant influence on the total amount of accumulated M^0.[49] However, in the presence of induced metal adsorption during the stripping step, the current-time transient is enhanced[3] leading to an increase in the analytical signal of nondepletive measurements.

Ligands are generally negatively charged, and since the typical initial potential values in SSV are negative of the potential of zero charge (*ca.* –0.5 V *vs.* SCE for Hg[50]), build-up of surface excess of ligand Γ_L and ensuing induced adsorption of M^{n+} as ML often becomes relevant only at the onset of the stripping process. The time constant for adsorption of L in the linear adsorption regime at a macroscopic (planar) electrode is given by K_H^2 / D for pure diffusion and $K_H \delta / D$ for convective diffusion.[50] Thus, Γ_L typically approaches its equilibrium value on a timescale of seconds, which is approximately the same as the effective measurement timescale operational during the reoxidation step of transient stripping techniques. The Anson equation[3] can be used to calculate the current-time transient following application

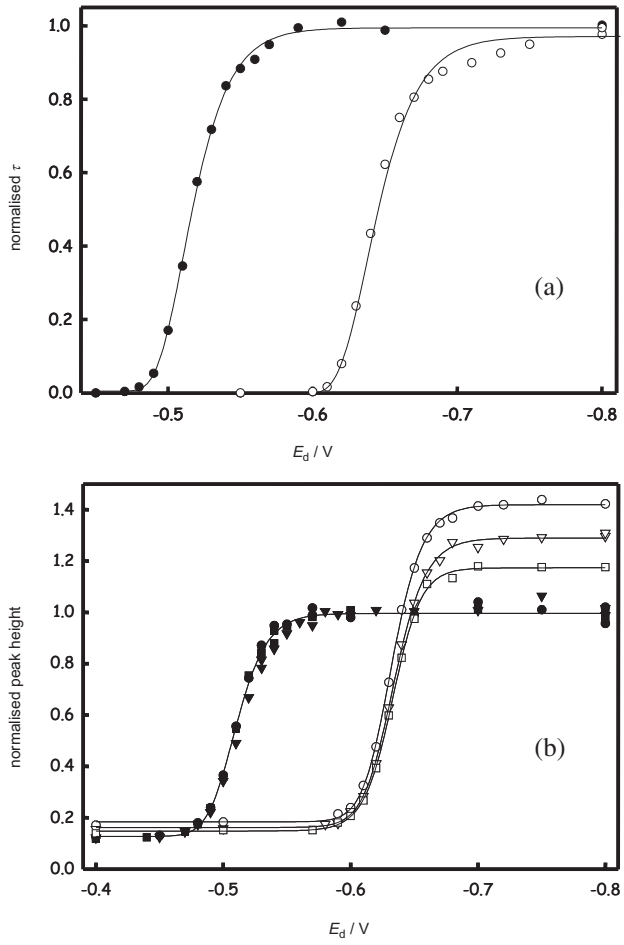

Figure 6. Comparison of experimental depletive SSCP and DP-SSV waves for the Pb^{II}-PDCA system (induced metal adsorption present). (a) depletive SSCP for Pb^{II} in the absence (●), and presence (○) of PDCA. (b) DP-SSV for Pb^{II} in absence (solid symbols) and presence (open symbols) of PDCA for a pulse amplitude of 5 mV (●,○), 20 mV (▼,▽), and 25 mV (■,□). Data are normalised with respect to the limiting peak magnitude for Pb^{II}-only. In each case data were measured at a HMDE ($A = 5.2 \times 10^{-7}$ m^2, $V = 3.5 \times 10^{-11}$ m^3), $c^*_{Pb^{II}} = 2 \times 10^{-7}$ mol dm^{-3}, $c^*_{PDCA} = 8.9 \times 10^{-5}$ mol dm^{-3} in 0.1 mol dm^{-3} KNO_3, pH = 4.8, T = 293 K, t_d = 60 s. SSCP: I_s of 2×10^{-9} A, applied from each E_d. DP-SSV: common initial potential of –0.80 V applied for duration of rest time (10 s); scan rate 16 mV s^{-1}.

of a potential step in the presence of adsorbing reactants and products that obey linear isotherms. The magnitude of the current enhancements depends on the relevant time scale parameter, as derived from the scan rate and/or modulation frequency. The shorter time scale DP and SW modes are the most greatly affected, with the impact dependent on the electrochemical parameters (*e.g.* modulation amplitude, frequency). Induced metal adsorption affects both the magnitude of the individual stripping peaks,[8] and the shape of the SSV wave.[41] SSCP and DP-SSV waves for the Pb^{II}-PDCA system demonstrate this effect; Figure 6. Free $PDCA^{2-}$ is not adsorbed on the Hg electrode under our experimental conditions,[8,62] whilst the metal complex adsorbs with K_H O(10^{-5}) m,[8] where

'O' denotes order of magnitude. The greatest impact of induced metal adsorption on DP-SSV waves is observed at the shortest pulse amplitude; DC-SV at slow scan rate is affected less, and the shorter timescale SW mode is affected more.[42]

In depletive SSCP, the reoxidation times are generally much greater than the time constant for adsorption of L, hence Γ_L corresponds to its equilibrium value over the entire transition period. Even if the extent of adsorption is not invariant with potential, the surface area of the depletive dt/dE curve contains no contribution from capacitive currents,[8] and the stripping peaks are practically not affected by induced metal adsorption, over the entire τ *vs.* E_d curve.[41]

Irreversible Electron Transfer

A system is irreversible when the charge transfer rate constant, k^o, is much lower than the diffusion rate constant, *i.e.* $k^o << \overline{D}/\delta$ for a macroelectrode and $k^o << \overline{D}/r_0$ for a microelectrode. Thus the minimum k^o necessary for an electrochemical reaction to be reversible at a microelectrode is greater than that at a macroelectrode. Eq. (1) for the complete SSCP wave still holds for irreversible systems, but with more involved expressions for τ_d and I_d^*:[34]

$$\tau_d = \frac{nFVm_M}{\theta} + \frac{V}{Ak^o\theta_\beta} \qquad (3)$$

$$I_d^* = \frac{nFAk^o}{1+nFAk^o m_M^* \exp(-\alpha y)} c_M^* \exp(-\alpha y) \qquad (4)$$

where $\theta = \exp[nF(E_d - E^{o'})/RT]$, $E^{o'}$ is the formal potential, m_M is a charge transport coefficient for M in solution (= $(1/\delta_M + 1/r_0)^{-1}/nFAD_M$), α is the electron transfer coefficient, $\beta = 1 - \alpha$, $\grave{e}_\beta = \exp(\beta y)$, and $y = nF(E - E^{o'})/RT$.

Following our approach, Omanović and Branica presented an analysis of SSV waves for such systems.[51] Both SSCP and SSV have a certain insensitivity to irreversibility, which, counterintuitive to traditional electrochemical reasoning, is even more pronounced at a microelectrode (see below).[34] Reversibility is lost mostly at the top of the scanned deposition potential wave. This feature is readily explained by the basic nature of the deposition step: when E_d is not sufficiently negative to drive c_M^0 to zero, the timescale for accumulation may be long enough for equilibrium to be attained between c_M^0 and $c_{M^0}^0$, and thus for irreversibility to be overcome. The relatively negative location of the SSCP and SSV waves on the E_d axis compounds this effect, consistent with conventional overcoming of irreversibility by going to more extreme potentials.

For quasireversible systems with electron rate transfer constants, k^o, between O(10^{-4}) to O(10^{-6}) m s^{-1}, the shape of the SSCP wave is dependent on the value of k^o, the deposition time, and the electrode size. So long as k^o remains the same in the presence of ligand (verifiable by observation of no change in the shape of the wave), the stability of a metal complex can be determined from the shift in $E_{d,1/2}$.[52] For completely irreversible systems, $k^o <$ O(10^{-7}) m s^{-1}, I_d becomes independent of time (Figure 1) and the SSCP wave shape is independent of k^o, t_d, and electrode size. Constancy of wave shape in the presence of a ligand is thus no longer a guarantee that k^o has not been modified. Nevertheless, if the metal reduction occurs at sufficiently negative potentials, then it is unlikely that negatively charged ligands will impact on k^o. This assumption has been observed to hold for Ni^{II}-citrate and -tartrate systems allowing the corresponding stability constants to be determined from the shift in $E_{d,1/2}$.[52] The expression for the shift in $E_{d,1/2}$ that incorporates all the preceding elements (formation of ML, reduced diffusion coefficient for ML, reduced lability of ML, and irreversibility in the electron transfer) is:

$$\Delta E_{d,1/2} = -\left[\frac{RT}{nF}[\ln(1+K') + \ln(\overline{D}/D_M)^p + \ln(\tau_{ML}/\tau_M) - \frac{RT}{\alpha nF}\ln(k^o_{complex}/k^o_{metal\text{-}only})\right] \qquad (5)$$

Eq. (5) is strictly limited to totally irreversible systems; quasireversible cases require a more involved expression that relates the rate of electron transfer to that of mass transport.

The transition from reversible to irreversible behaviour depends on the timing characteristics of the technique, which for depletive SSCP corresponds to k^o values in the range from about 10^{-4} to 10^{-6} m s^{-1}. For modulated SV techniques the relevant timescale is the pulse duration for DP, and the inverse frequency for SW. Zn^{II} reduction becomes more irreversible as the concentration of supporting electrolyte is increased: reported k^o values for 1.0 mol dm^{-3} KNO_3 are in the range from 2.8 to 4.2 × 10^{-5} m s^{-1}, and $\alpha \approx 0.3$.[53–56] For this system the scanned deposition potential waves recorded by SCP (depletive and nondepletive), DP-SV (modulation time 0.01 s), and SW-SV (frequency range 50 to 1000 Hz) all had a similar shape at the more negative E_d values. The results are consistent with that predicted by Eq. (1), incorporating Eqs. (3) and (4), *i.e.* k^o corresponds to quasireversible behaviour for this range of timescales.[34] The depletive SSCP wave maintained reversible behaviour to slightly more negative E_d than did the other modes, suggesting that there is some limitation arising from the rate of oxidation for the faster modes.

The Ni^{II}/Ni(Hg) system is irreversible: k^o has been reported as 1 × 10^{-12} m s^{-1} in 0.1 mol dm^{-3} KNO_3, with

α = 0.4. As expected, the depletive SSCP wave has the same form as a conventional voltamogram (Figure 2).[52] No meaningful measurements of Ni^{II} could be made by DP-SV or SW-SV: the sensitivity was very low (*e.g.* DP-SV peak current *ca.* 20 times less than that for DC-SV for a similar potential scan rate) and multiple peaks were observed. These limitations observed for the faster timescale nondepletive stripping methods are ascribed to a combination of (i) the irreversibility of the electrochemical reaction, (ii) the low solubility of Ni^0 in Hg and its tendency to form stable amalgam compounds[58] (longer timescale methods allow time for a certain dissolution of any solid phase formed; see above), and (iii) the low diffusion coefficient of Ni^0 in Hg (5.4×10^{-10} m^2 s^{-1} at 298 K[58]).

Heterogeneity in the Metal Speciation

Many ligands present in environmental and biological media are chemically heterogeneous, as exemplified by humic substances. In the presence of such complexants, SSCP waves are spread along the E_d axis and the reciprocal log slope is decreased relative to the homogenous case; Figure 7.[41,59] This effect has also been observed by conventional voltammetry,[60] and can be ascribed to the range of metal complexes present, with different stabilities and mobilities. For SSCP the impact of heterogeneity is independent of t_d and electrode size, thus allowing this feature to be unambiguously identified. Depletive SSCP is the method of choice for such systems because it is not affected by the induced metal adsorption that is typically present (see above),[61–64] nor by ligand saturation at the electrode surface during reoxidation. The requirement for excess ligand strictly applies to every component of the mixture,[65] which is a very restrictive condition for nondepletive SV modes.

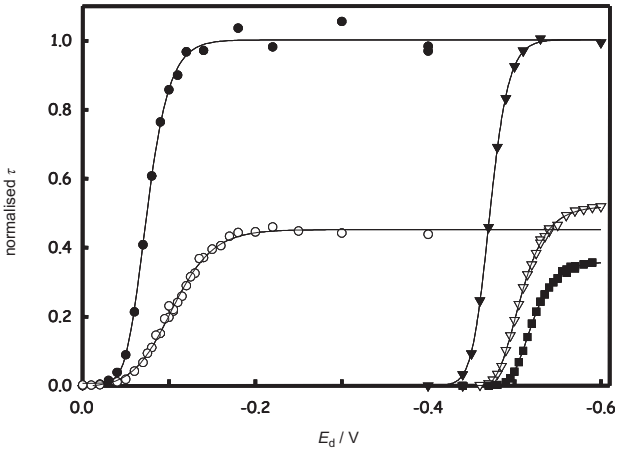

Figure 7. Experimental depletive SSCP waves for Cu^{II} and Pb^{II} peat FA systems. Data are shown for Cu^{II} in the absence (●) and presence (○) of 1.5 mg FA dm^{-3}, and for Pb^{II} in the absence (▼) and presence of 15 mg FA dm^{-3} (▽) and 58 mg FA dm^{-3} (■). Conditions: HMDE ($A = 5.2 \times 10^{-7}$ m^2, $V = 3.5 \times 10^{-11}$ m^3), t_d = 180 s, $I_s = 2 \times 10^{-9}$ A, $c^*_{M^{II}} = 2 \times 10^{-7}$ mol dm^{-3} in 0.1 mol dm^{-3} KNO_3, pH = 4.8, T = 293 K. Data are normalised with respect to the limiting τ for the metal-only wave in each case.

Rigorous quantification of heterogeneity via SSCP or SSV is practically impossible because a measurement at a given E_d does not conform to a fixed surface concentration of metal ion (c^0_M is a function of time) and thus the relative proportion of complexes contributing to the flux is not fixed. Furthermore, the precise meaning of the shift in $E_{d,1/2}$ upon complexation is not well defined for heterogeneous systems because $\overline{D}$ and the average stability constant, $\overline{K}$, become a function of position inside the steady-state diffusion layer. Nevertheless the slope of the SSCP wave contains unambiguous information on the extent of heterogeneity of the complex species present, and clear differences are observed between metal ions (Figure 7). We observe a relative heterogeneity order of Cd< Pb < Cu,[59] consistent with results from potentiometric titrations.[66] We have established the first foundations for interpretation of heterogeneous complexation parameters from SSCP waves, including the impact of kinetic currents, based on the Freundlich isotherm and the Koutecký-Koryta approximation.[59] The derived expression provides a good description of the experimental data for moderate degrees of heterogeneity (Cd^{II} and Pb^{II} complexes).

Special Features of Microelectrode Measurements

For a microelectrode, $r_0 < \delta_M$, the radial term governs the deposition flux and steady-state is attained within a very short time, $O(r_0^2 / D)$. In practice, the diffusive flux can be considered to be essentially steady-state. Thus the applicability of Eq. (1) over the entire accumulation period is even better at a microelectrode than at a macroscopic one. For reversible systems, the shape of an SSCP wave recorded at a microelectrode is the same as that at a HMDE (Figure 2). During the reoxidation step, the characteristic time constant for diffusion of metal over the effective electrode dimension is also much faster at a microelectrode (*ca.* 10^{-1} s) than at a conventional HMDE (*ca.* 20 s), meaning that the steady-state M^0 concentration profile inside the electrode is attained more rapidly.

The time dependence of adsorption processes at a microelectrode is reduced relative to the macroelectrode, even for transient techniques, *e.g.* DP-SV. This is so because, as compared to the case of convective diffusion at a macroelectrode, the adsorption process is more rapid, and the time constant for adsorption of ligand is reduced by a factor of *ca.* 100, to *ca.* 0.05 s (for $r_0 = 5 \times 10^{-6}$ m, $K_H = 10^{-5}$ m). This compares with a typical pre-pulse period of O(1) s in DP-SV, meaning that during the stripping step at a microelectrode the surface excess of L will be close to its equilibrium value.

Depletive SSCP waves recorded at a microelectrode exhibit greater resistance to irreversibility than at a

HMDE. This is because the waves lie to more negative potentials on the E_d axis due to higher concentration of reduced metal in the small electrode volume. Therefore, for a given k^o and t_d the SSCP wave is relatively steeper at the microelectrode and this disparity is enhanced as k^o decreases (Figure 2). This striking feature is of importance for *in situ* analysis of natural waters where microelectrodes are typically required.

Compared to the macroelectrode, microelectrode SSCP is less susceptible to interferences from the electroless oxidation that can arise in multi-metal systems. This is due to the application of higher stripping current densities, and the greater concentration of reduced metal in the small electrode volume as compared to a HMDE. Thus, for a given bulk concentration of the less electropositive metal ion in solution, the ratio between its flux towards the electrode and the reoxidation flux of the more electropositive ion, generated by I_s, is greater at the microelectrode.[11]

For systems influenced by homogeneous kinetics, the transition from a macro- to a microelectrode influences the relative contributions of diffusion and kinetic fluxes to the overall mass transport to the surface and thus the extent of lability of metal complex species. The lability of metal complex species is reduced at a microelectrode due to enhanced diffusion.[9,35,67]

Due to the different dependencies of various chemical speciation features on the electrode size, measurements at micro- and macroelectrode are complementary for unambiguous identification of, *e.g.*, irreversibility *vs.* heterogeneity.

CONCLUSIONS

Depletive stripping modes have significant advantages over transient methods for construction of scanned deposition potential waves. When effectively all the accumulated metal is stripped from the electrode there is a straightforward relationship between the analytical signal and the amount of metal accumulated and the stripping signals are not affected by induced metal adsorption. The slow rate of oxidation also confers greater resistance to irreversibility in the electrochemical reaction and to formation of intermetallic compounds. The enhanced diffusion at microelectrodes confers special properties, and measurements at macro- and microelectrodes provide complementary information. By systematic variation of t_d and electrode size, dynamic speciation characteristics can be unambiguously identified and discriminated from features due to irreversibility in the electrochemical reaction or heterogeneity in the chemical speciation.

In many cases depletive SSCP is the method of choice because it has better resolution and greater sensitivity than slow-scan DC-SV. Practical recording of the SSCP wave avoids the need to use a common 'initial potential' prior to each reoxidation step. In multi-metal systems, SSV is a useful complement to SSCP for identification of electroless oxidation processes. It is worth noting that medium-exchange[68] would overcome some of the stripping step complications of SSV (requirement for ligand excess and induced metal adsorption) and would avoid electroless oxidation in SSCP. However, this approach has proven technically difficult to implement in practice, and it cannot get around irreversibility in the electrochemical oxidation, nor intermetallic compound effects.

SYMBOLS AND ABBREVIATIONS

A/m^2	electrode surface area
α	electron transfer coefficient
c^*_M/mol dm^{-3}	concentration of metal ion in the bulk solution
c^0_M/mol dm^{-3}	concentration of metal ion at the electrode surface
$c^*_{M^0}$/mol dm^{-3}	concentration of reduced metal in the electrode volume
$c^0_{M^0}$/mol dm^{-3}	concentration of reduced metal at the electrode surface
D/m^2 s^{-1}	diffusion coefficient
δ/m	diffusion layer thickness
DC	direct current
DP	differential pulse
E_d/V	deposition potential
$E_{d,1/2}$/V	half-wave deposition potential
Γ	degree of surface coverage
HMDE	hanging mercury drop electrode
I^*_d/A	limiting value of the deposition current
k^o/m s^{-1}	charge transfer rate constant
K_H/m	Henry coefficient
K/dm^3 mol^{-1}	stability constant
μ/m	reaction layer thickness
r_0/m	spherical radius of microelectrode
SCP	stripping chronopotentiometry
SSCP	scanned (deposition potential) stripping chronopotentiometry
SV	stripping voltammetry
SSV	scanned (deposition potential) stripping voltammetry
SW	square wave
τ/s	SCP transition time
τ_d/s	time constant for deposition
t_d/s	deposition time
V/m^3	electrode volume

Acknowledgements. – This work was performed within the framework of the BIOSPEC project funded by the European Commission's RTD Programme »Preserving the Ecosystem« (Key Action Sustainable Management and Quality of Water), under contract EVK1-CT-2001-00086.

REFERENCES

1. J. Buffle and M.-L. Tercier-Waeber, In Situ *Voltammetry: Concepts and Practice for Trace Analysis and Speciation*, in: J. Buffle and G. Horvai (Eds.), In Situ *Monitoring of Aquatic Systems: Chemical Analysis and Speciation*, IUPAC Series on Analytical and Physical Chemistry of Environmental Systems, Vol. 6, J. Buffle and H. P. van Leeuwen (Series Eds.), Wiley, Chichester, 2000, pp. 279–405.
2. R. M. Town and H. P. van Leeuwen, *J. Electroanal. Chem.* **509** (2001) 58–65.
3. F. C. Anson, J. B. Flanagan, K. Takahasi, and A. Yamada, *J. Electroanal. Chem.* **67** (1976) 253–259.
4. J. Buffle, *J. Electroanal. Chem.* **125** (1981) 273–294.
5. A. M. A. Mota, J. Buffle, S. P. Kounaves, and M. L. S. Gonçalves, *Anal. Chim. Acta* **172** (1985) 13–30.
6. R. M. Town and H. P. van Leeuwen, *J. Electroanal. Chem.* **535** (2002) 11–25.
7. N. Serrano, J. M. Díaz-Cruz, C. Ariño, and M. Esteban, *J. Electroanal. Chem.* **560** (2003) 105–116.
8. R. M. Town and H. P. van Leeuwen, *J. Electroanal. Chem.* **523** (2002) 1–15.
9. H. P. van Leeuwen and R. M. Town, *J. Electroanal. Chem.* **523** (2002) 16–25.
10. H. P. van Leeuwen and R. M. Town, *J. Electroanal. Chem.* **535** (2002) 1–9.
11. R. M. Town and H. P. van Leeuwen, *J. Electroanal. Chem.* **573** (2004) 147–157.
12. H. P. van Leeuwen and J. Buffle, *J. Electroanal. Chem.* **296** (1990) 359–370.
13. S. Bubić and M. Branica, *Thalassia Jugosl.* **9** (1973) 47–53.
14. D. D. DeFord and D. N. Hume, *J. Am. Chem. Soc.* **73** (1951) 5321–5322.
15. M Branica, I. Pižeta, and I. Marić, *J. Electroanal. Chem.* **214** (1986) 95–102.
16. D. Omanović and M. Branica, *J. Electroanal. Chem.* **543** (2003) 83–92.
17. S. D. Brown and B. R. Kowalski, *Anal. Chem.* **51** (1979) 2133–2139.
18. H. W. Nürnberg, *Potentialities of Voltammetry for the Study of Physicochemical Aspects of Heavy Metal Complexation in Natural Waters,* in: C. J. M. Kramer and J. C. Duinker (Eds.), *Complexation of Trace Metals in Natural Waters*, Martinus Nijhoff/Dr W. Junk, The Hague, 1984, pp. 95–115.
19. M. Branica, D. M. Novak, and S. Bubić, *Croat. Chem. Acta* **49** (1977) 539–547.
20. D. L. Huizenga and D. R. Kester, *J. Electroanal. Chem.* **164** (1984) 229–236.
21. Š. Komorsky-Lovrić, M. Lovrić, and M. Branica, *J. Electroanal. Chem.* **214** (1986) 37–50.
22. D. Omanović and M. Branica, *Croat. Chem. Acta* **71** (1998) 421–433.
23. F. Eyrolle, D. Fevrier, and J.-Y. Benaim, *Environ. Technol.* **14** (1993) 701–717.
24. M. T. Lam, C. L. Chakrabarti, J. Cheng, and V. Pavski, *Electroanalysis* **9** (1997) 1018–1029.
25. B. L. Lewis, G. W. Luther, H. Lane, and T. M. Church, *Electroanalysis* **7** (1995) 166–177.
26. P. L. Croot, J. W. Moffett, and G. W. Luther, *Mar. Chem.* **67** (1999) 219–232.
27. J. A. Wise, D. A. Roston, and W. R. Heineman, *Anal. Chim. Acta* **154** (1983) 95–104.
28. H. P. van Leeuwen, H. G. De Jong, and K. Holub, *J. Electroanal. Chem.* **260** (1989) 213–220.
29. H. P. van Leeuwen, *Sci. Total Environ.* **60** (1987) 45–55.
30. M.-L. Tercier-Waeber and J. Buffle, *Environ. Sci. Technol.* **34** (2000) 4018–4024.
31. W. T. De Vries, *J. Electroanal. Chem.* **9** (1965) 448–456.
32. W. T. De Vries and E. van Dalen, *J. Electroanal. Chem.* **14** (1967) 315–327.
33. H. P. van Leeuwen and R. M. Town, *J. Electroanal. Chem.* **536** (2002) 129–140.
34. H. P. van Leeuwen and R. M. Town, *J. Electroanal. Chem.* **556** (2003) 93–102.
35. H. P. van Leeuwen and R. M. Town, *J. Electroanal. Chem.* **561** (2004) 67–74.
36. M. S. Shuman and J. L. Cromer, *Anal. Chem.* **51** (1979) 1546–1550.
37. A. Zirino and S. P. Kounaves, *Anal. Chem.* **49** (1977) 56–59.
38. S. P. Kounaves, *Anal. Chem.* **64** (1992) 2998–3003.
39. M. Lovrić, *Electroanalysis* **10** (1998) 1022–1025.
40. E. Sahlin and D. Jagner, *Electroanalysis* **10** (1998) 532–535.
41. R. M. Town and H. P. van Leeuwen, *J. Electroanal. Chem.* **541** (2003) 51–65.
42. R. M. Town and H. P. van Leeuwen, *Electroanalysis* **16** (2004) 458–471.
43. J. Heyrovský and J. Kuta, *Principles of Polarography*, Academic Press, New York, 1966.
44. J. Koutecký and J. Koryta, *Electrochim. Acta* **3** (1961) 318–339.
45. J. Koryta, J. Dvorak, and L. Kavan, *Principles of Electrochemistry*, 2nd edn., Wiley, Chichester, 1993.
46. H. P. van Leeuwen, J. Puy, J. Galceran, and J. Cecília, *J. Electroanal. Chem.* **526** (2002) 10–18.
47. J. Galceran, J. Puy, J. Salvador, J. Cecília, and H. P. van Leeuwen, *J. Electroanal. Chem.* **505** (2001) 85–94.
48. J.-P. Pinheiro and H. P. van Leeuwen, *J. Electroanal. Chem.* **570** (2004) 69–75.
49. D. Omanović and M. Lovrić, *Electroanalysis* **16** (2004) 563–571.
50. A. J. Bard and L. R. Faulkner, *Electrochemical Methods. Fundamentals and Applications*, 2nd ed., Wiley, New York, 2001.
51. D. Omanović and M. Branica, *J. Electroanal. Chem.* **565** (2004) 37–48.
52. R. M. Town, J.-P. Pinheiro, R. Dominogos, and H. P. van Leeuwen, *J. Electroanal. Chem.* **580** (2005) 57–67.
53. W. S. Go, J. J. O'Dea, and J. Osteryoung, *J. Electroanal. Chem.* **255** (1988) 21–44.
54. J. Koryta, *Electrochim. Acta* **6** (1962) 67–74.
55. N. Tanaka and R. Tamamushi, *Electrochim. Acta* **9** (1964) 963–989.
56. R. L. Birke, M.-H. Kim, and M. Strassfeld, *Anal. Chem.* **53** (1981) 852–856.
57. K. Morinaga, *Bull. Chem. Soc. Jpn.* **29** (1956) 793–799.
58. A. BaraZski and Z. Galus, *J. Electroanal. Chem.* **46** (1973) 289–305.
59. R. M. Town and H. P. van Leeuwen, *Aust. J. Chem.* **57** (2004) 983–992.

60. H. P. van Leeuwen and J. Buffle, *J. Electroanal. Chem.* **296** (1990) 359–370.
61. J. Buffle and F.-L. Greter, *J. Electroanal. Chem.* **101** (1979) 231–251.
62. J. Buffle, A. M. Mota, and M. L. S. Gonçalves, *J. Electroanal. Chem.* **223** (1987) 235–262.
63. M. Plavšić and B. Ćosović, *Mar. Chem.* **36** (1991) 39–49.
64. J. P. Pinheiro, A. M. Mota, M. L. S. Gonçalves, M. van der Weijde, and H. P. van Leeuwen, *J. Electroanal. Chem.* **410** (1996) 61–68.
65. J. Buffle, *Complexation Reactions in Aquatic Systems. An Analytical Approach*, Ellis Horwood, Chichester, 1988.
66. D. G. Kinniburgh, C. J. Milne, M. F. Bennedetti, J. P. Pinheiro, J. Filius, L. K. Koopal, and W. H. van Riemsdijk, *Environ. Sci. Technol.* **30** (1996) 1687–1698.
67. J. Galceran, J. Puy, J. Salvador, J. Cecília, and H. P. van Leeuwen, *J. Electroanal. Chem.* **505** (2001) 85–94.
68. T. M. Florence and K. J. Mann, *Anal. Chim. Acta* **200** (1987) 305–312.

SAŽETAK

Usporedna procjena oksidacije amalgama kronopotenciometrijom i voltametrijom

Raewyn M. Town i Herman P. van Leeuwen

Kritički su procijenjena karakteristična svojstva pseudopolarograma konstruiranih korištenjem dvaju metoda oksidacije amalgama: kronopotenciometrije i voltametrije. Pseudopolarogram je prikaz ovisnosti najvećeg intenziteta odziva oksidacije amalgama o potencijalu redukcije metalnih iona. Opisane su prednosti i mane obaju metoda pri određivanju raspodjele metalnih kompleksa i njihova podložnost tipičnim smetnjama. Analizirani su odzivi na visećoj živinoj kapi i na mikroelektrodama. Razmatrane su sljedeće pojave: reverzibilnost i brzina prijenosa elektrona, razdvajanje odziva većeg broja metala u živi, stvaranje intermetalnih spojeva u živi, utjecaji kemijskih reakcija koje prethode redukciji metalnih iona ili slijede oksidaciju amalgama, inducirana adsorpcija metalnih iona na površinu živine elektrode i minimalni višak slobodnog liganda potreban da se tijekom oksidacije amalgama svi metalni ioni uz površinu elektrode odmah kompleksiraju. Najbolja metoda oksidacije jest ona kojom se postiže potpuna oksidacija svih metalnih atoma akumuliranih u živi. Taj uvjet zadovoljavaju kronopotenciometrija sa slabom strujom i voltametrija sa sporom promjenom potencijala. Pod tim uvjetima postoji kvantitativna funkcionalna veza intenziteta odziva i količine akumuliranih metalnih atoma. Metode spore oksidacije su imune na induciranu adsorpciju, trebaju manji višak slobodnog liganda, manje ovise o brzini izmjene elektrona i manje im smetaju intermetalni spojevi. Ovim metodama mogu se odrediti konstante stabilnosti metalnih kompleksa i u slučajevima kinetički kontroliranih elektrodnih reakcija i sporih reakcija kompleksiranja ili disocijacije kompleksa. Pokazano je da je kronopotenciometrija osjetljivija od voltametrije i da se njenim korištenjem postiže bolja rezolucija odziva većeg broja metala, ali se voltametrijom mogu dobiti dodatne informacije o istraživanom sustavu.